Quantitative Analysis on Boundary Sliding and Its Accommodation Mode during Superplastic Deformation of Two-Phase Ti-6Al-4V Alloy

JI SIK KIM, YOUNG WON CHANG, and CHONG SOO LEE

A study has been made to investigate boundary sliding and its accommodation mode with respect to the variation of grain size and α/β volume fraction during superplastic deformation of a two-phase Ti-6Al-4V alloy. A load relaxation test has been performed at 600 °C and 800 °C to obtain the flow stress curves and to analyze the deformation characteristics by the theory of inelastic deformation. The results show that grain matrix deformation (GMD) is found to be dominant at 600 °C and is well described by the plastic state equation. Whereas, at 800 °C, phase/grain boundary sliding (P/GBS) becomes dominant and is fitted well with the viscous flow equation. The accommodation mode for fine-grained microstructures (3 μm) well agrees with the isostress model, while that for large-grained structures (11 μm) is a mixed mode of the isostress and isostrain-rate models. The sliding resistance analyzed for the different boundaries is lowest in the α/β boundary, and increases on the order of $\alpha/\beta << \alpha/\alpha \approx \beta/\beta$, which plays an important role in controlling the superplasticity of the alloys with various α/β phase ratios.

I. INTRODUCTION

SINCE manufacturing costs and the weight of airframe structures can be reduced significantly through superplastic forming technology,[1] considerable efforts have been devoted during the past three decades to the investigation of the superplastic deformation behavior of various metallic alloys, especially the Ti-6Al-4V alloy. As a result, the role of several microstructural features such as grain size,[2] grain size distribution,[3] grain growth,[4] texture,[5] and volume fraction of the component phase[6–9] have been well established in relation to the actual forming process of the Ti-6Al-4V alloy. Nowadays, many components of airframe structures are being produced by superplastic forming of the Ti-6Al-4V alloy, and its commercial applications are expected to increase.[10]

In contrast to the commercial success of the superplasticity of Ti-6Al-4V alloys, a satisfactory explanation of the mechanism for this deformation phenomenon is still not available. Although many investigations have been carried out on the mechanisms of superplastic deformation of two-phase alloys,[11,12,13] there remain two major, vague points. First, in the case of two-phase alloys like Ti-6Al-4V, boundary slidings take place at the grain boundary and the phase boundary concurrently. While several efforts have been made to understand the resistance of the boundary slidings either by measuring the sliding displacement of the surface[14,15] or the flow stress of the bicrystal,[16,17] relative sliding resistance between the grain boundary and the phase boundary have not been quantified yet. Second, there has been an evident controversy over the deformation modes[7,8,9] of accommodation, which can be classified as the isostress mode and the isostrain-rate mode. It is important to determine the deformation modes in relation to the α/β volume ratio and the grain size. In order to clarify the aforementioned points, more fundamental analysis considering the physical characteristics of superplastic deformation has to be made.

The present article, therefore, attempts to analyze the superplastic deformation behavior of the Ti-6Al-4V alloy based on the inelastic deformation theory[18] in two aspects: one is to investigate the relative sliding characteristics at each type of boundary and the other is to verify the deformation mode of accommodation. For this purpose, the flow characteristics of the Ti-6Al-4V alloy with respect to the variation of α/β volume fraction are studied by load relaxation tests. In the following section, an inelastic deformation theory,[18] which consists of two mechanisms, *i.e.*, grain matrix deformation (GMD) and grain boundary sliding (GBS), is briefly described.

II. INELASTIC DEFORMATION THEORY

A simple rheological and topological model for GMD and phase/GBS (P/GBS) has been proposed by Chang and Aifantis[18] and is schematically shown in Figure 1. The model represents that P/GBS is mainly accommodated by a dislocation process giving rise to an internal strain rate ($\dot{a}$) and plastic strain rate ($\dot{\alpha}$). A more detailed description of $\dot{a}$ and $\dot{\alpha}$ is given in Reference 18.

For the model given in Figure 1, we have the following stress relation and kinematic relation among the deformation rate variables $\dot{a}$ and $\dot{\alpha}$ and the P/GBS rate $\dot{g}$:

$$\sigma = \sigma^I + \sigma^F \quad [1]$$

$$\dot{\varepsilon} = \dot{a} + \dot{\alpha} + \dot{g} \quad [2]$$

The stress variables σ^I and σ^F are the internal stress due to a long-range interaction among dislocations and the friction stress due to short-range interaction between dislocation

JI SIK KIM, Graduate Research Assistant, YOUNG WON CHANG, Professor, and CHONG SOO LEE, Associate Professor, are with the Center for Advanced Aerospace Materials, Pohang University of Science and Technology, Pohang 790-784, Korea.

Manuscript submitted June 2, 1997.

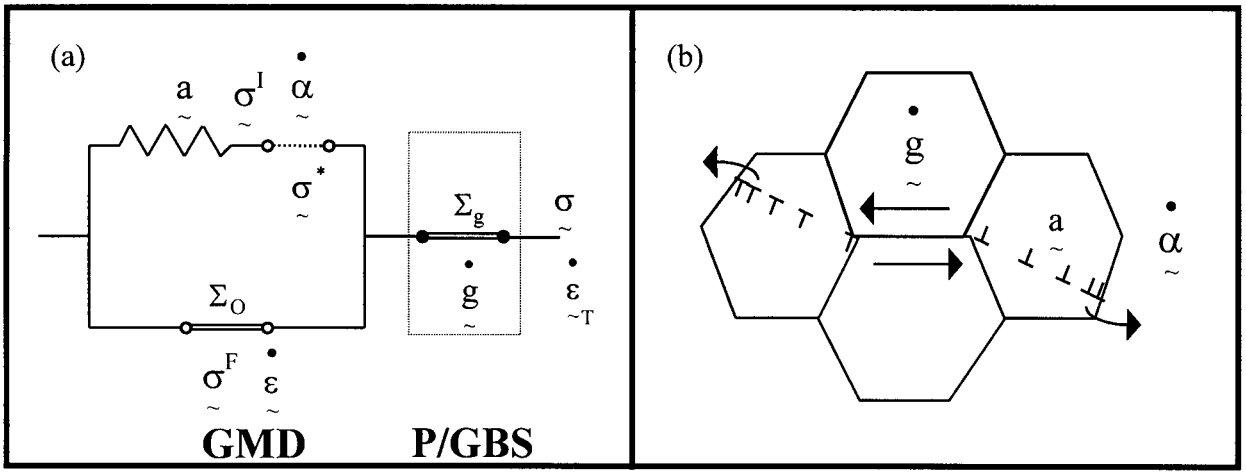

Fig. 1—An internal variable model for describing the structural superplasticity: (*a*) a rheological model and (*b*) a topological model.

and lattice, respectively. The symbol ° above *a* denotes the material's time rate of change; *a* is corotational tensor of internal strain.[19]

At the high-temperature range used in this study, σ^F is, in general, very small as compared to σ^I, and $\mathring{a}$ can be neglected if the relaxation test is performed at a steady state. It is, therefore, sufficient to describe the constitutive relation using only the $\mathring{a}$ and $\dot{g}$ elements of Figure 1 at high temperatures. The constitutive relation between σ^I and $\dot{\alpha}$ can be expressed, in a form similar to that by Hart,[20] as

$$(\sigma^*/\sigma^I) = \exp\,(\dot{\alpha}^*/\dot{\alpha})^P \qquad [3]$$

$$\dot{\alpha}^* = f^I\,(\sigma^*/\mu)^{n^I} \exp\,(-\,Q^I/RT) \qquad [4]$$

where p and n^I are the material constants and σ^* and $\dot{\alpha}^*$ are the internal strength variable and its conjugate reference strain rate, respectively. Equation [4] represents an activation relation for dislocations at grain boundaries, with f^I denoting jump frequency, Q^I activation energy, and μ an internal modulus.

Considering P/GBS as a viscous drag process similar to the frictional glide process of dislocations, the following power-law relations can be described for GBS:

$$(\dot{g}/\dot{g}_0) = \exp\,(\sigma/\Sigma_g - 1)^{1/M_g} \qquad [5]$$

$$\dot{g}_0 = f^g\,(\Sigma_g/\mu_g)^{ng} \exp\,(-\,Q^g/RT) \qquad [6]$$

where M_g is a material constant and Σ_g and $\dot{g}_0$ are the static friction stress and its conjugate reference rate for P/GBS, respectively. Equation [6] also represents a thermally activated process of GBS, with Q^g now denoting the activation energy for P/GBS.

III. EXPERIMENTAL PROCEDURE

The Ti-6Al-4V alloy was supplied by Timet (Henderson, NV) in a plate form of 25-mm thickness. The chemical composition is shown in Table I. The microstructure of the as-received material showed a Widmanstätten-type structure over the entire material. To obtain a fine equiaxed grain microstructure, the thermomechanical processing method developed by Peters[21] was applied. The plate was homogenized at 1050 °C for 30 minutes and cross-rolled from 25 to 12 mm to avoid the formation of contiguous α. After the final deformation, the material was recrystallized at 900 °C for 1 and 24 hours to obtain the grain sizes of 3 and 11 μm, respectively, and then annealed at 875 °C, 900 °C, and 925 °C for 1 hour to change the α/β volume fraction. Typical microstructures upon annealing at 875 °C, 900 °C, and 925 °C after 1 hour recrystallization are shown in Figure 2, indicating that the β volume fraction is increased to 34, 48, and 64 pct with the increase of annealing temperature. The microstructural parameters for the specimens annealed at different temperatures are summarized in Table II.

Table I. Chemical Composition of Ti-6Al-4V Plate

Alloy	Al	V	Fe	O	N	C	H	Ti
Wt pct	6.4	4.0	0.14	0.14	0.015	0.012	0.004	bal

Load relaxation tests were used to evaluate flow stress characteristics with variation of the α/β volume fraction (34, 48, and 64 pct β) and grain size (3 and 11 μm). The tests were carried out in an Ar atmosphere at two different temperatures: one at 600 °C where creep due to GMD would prevail, and the other at 800 °C where both GMD and GBS would operate at the same time. Round specimens with a gage diameter of 6 mm and a gage length of 15 mm were used for the tests. The flow stress and inelastic strain rates obtained by load relaxation tests were analyzed by the nonlinear regression method of a commercial curve-fit program. Tensile tests were performed using plate-type specimens with a gage dimension of 15-mm length, 4-mm width, and 2.5-mm thickness to estimate the amount of surface displacement of each type of boundary (α/α, α/β, and β/β) produced during the deformation at 800 °C.

All the mechanical tests at high temperatures were conducted on an automated static machine (Instron 1361) equipped with a 5 kW radiant heating system. Due to the fast response of the radiant heating (200 °C/min) and the short period and small strain of the load relaxation tests (2 to 5 minutes at 800 °C, 5 to 10 minutes at 600 °C, and $\varepsilon = 0.02$ to 0.03), the nonequilibrium microstructures with different α/β phase ratios were not significantly changed before and after the load relaxation tests, which was evidenced by microstructural analysis.

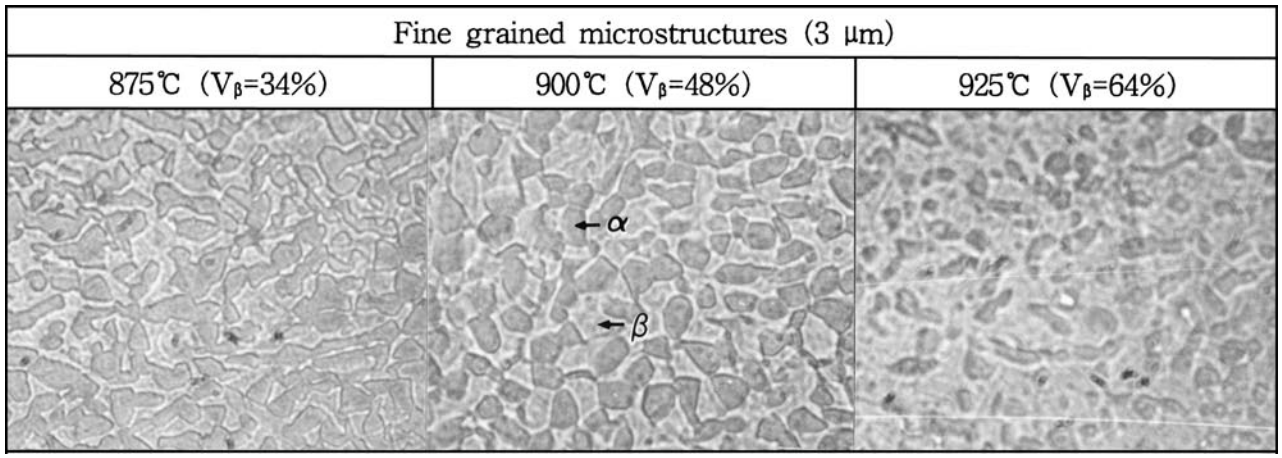

(*a*)

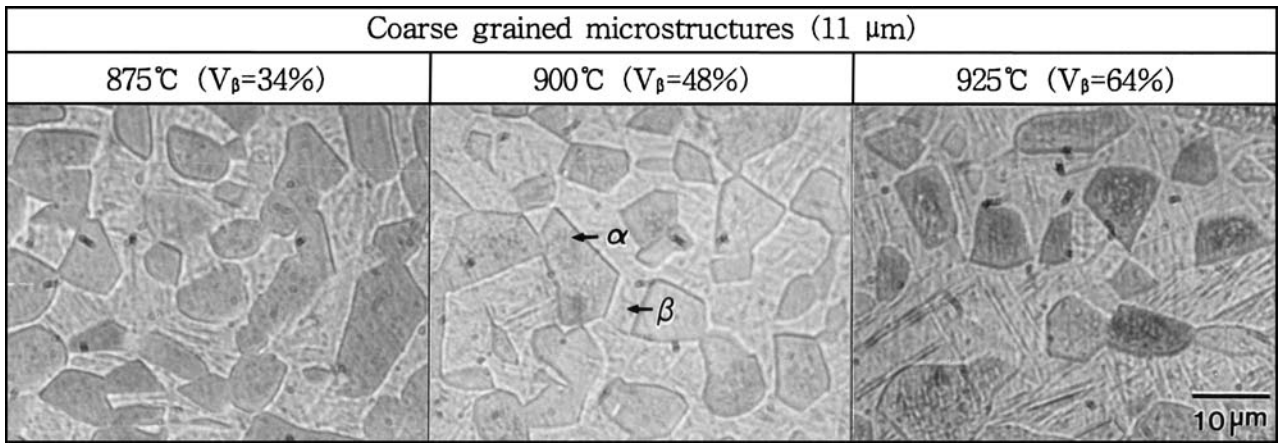

(*b*)

Fig. 2—Optical micrographs showing the microstructures annealed at 875 °C, 900 °C, and 925 °C for 1 h: (*a*) fine-grained microstructure (3 μm) and (*b*) coarse-grained microstructures (11 μm).

IV. RESULTS

A. *Flow Behavior at 600 °C with the Variation of α/β Phase Ratio and Grain Size*

The results of load relaxation tests at 600 °C for fine- (3 μm) and coarse- (11 μm) grained microstructures are shown in Figure 3. From the shape of the curves, GMD such as dislocation creep is considered to be predominant at this temperature. It is apparent that, as the volume fraction of β phase increases, the flow stress decreases in both fine- and coarse-grained microstructures. It is not surprising to observe this trend, since the bcc, β phase has more slip systems than the hcp α phase, and the diffusivity of β phase is about two orders of magnitude higher than that of the α phase.[7] However, it is noted that the variation of flow stress curves with equal β volume fraction is different for small- and large-grain-size specimens. In the case of small-grained materials (Figure 3(a)), the decrease of flow stress is more obvious at a low strain rate, but, in the large-grained materials (Figure 3(b)), the reverse is true. This difference might imply that the matrix deformation modes (isostress or isostrain-rate mode) operating in these two microstructures are different. This is further analyzed in Section V. Figure 3 also represents the general grain-size effect at 600 °C, which is that the coarse-grained material represents higher flow stress than the fine-grained material.

Table II. Microstructural Parameters of the Annealed Structures at 875 °C, 900 °C, and 925 °C after 1- and 24-Hour Recrystallization

	Annealing Temperature (°C)		
Parameter	875	900	925
	1-hour recrystallization		
Mean grain size (μm)	2.75	3.23	3.1
Volume fraction of β (pct)	34 pct	48 pct	64 pct
	24-hour recrystallization		
Mean grain size (μm)	10.25	10.62	11.27
Volume fraction of β (pct)	34 pct	48 pct	64 pct

To examine the deformation characteristics of the Ti-6Al-4V alloy at 600 °C by use of the internal-state variables, the plastic-state equation (Eq. [3]) describing GMD has been applied. The solid lines in Figure 3 are the predicted lines from Eq. [3] using the constitutive parameters obtained by the nonlinear regression method, as shown in Table III, and are well fitted to the experimental results with an exponent (p) of 0.15. The parameter p characterizes the

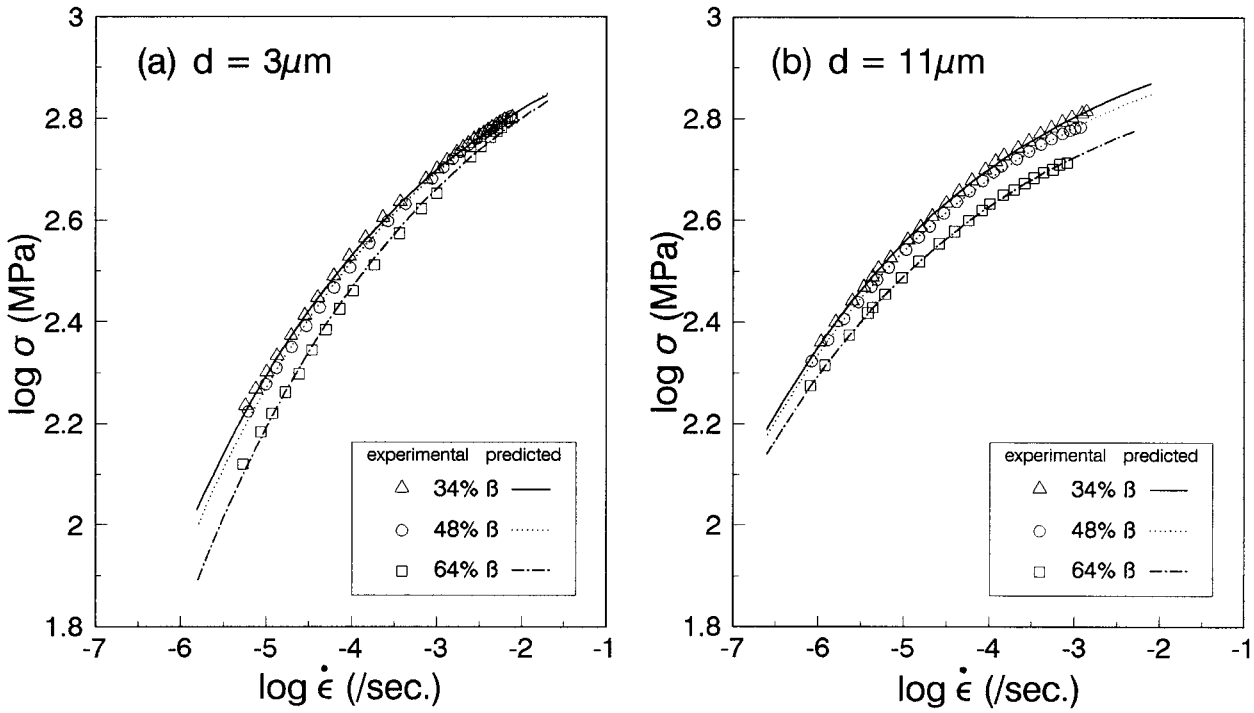

Fig. 3—Effects of β volume fraction on the flow stress curves for the GMD at 600 °C: (*a*) 3-μm microstructure and (*b*) 11-μm microstructure.

dislocation permeability through the barriers (grain boundary, phase boundary, *etc.*), and, thus, depends strongly on the barrier properties, including its geometry and structure. In the previous works,[22] the material parameter p has been determined as 0.15 for most of the cubic and hexagonal structures, except for the tetragonal structure.[23] Therefore, it is natural to observe that the permeability parameter of the Ti-6Al-4V alloy composed of hcp and bcc phases is constant (0.15), although the α/β volume fraction is varied in the microstructure. Table III also represents the values of two important state variables (σ^* and $\dot{\alpha}^*$) for different α/β volume fractions, which vary with the β volume fraction, in an opposite manner, between the fine- and coarse-grained materials.

Table III. Constitutive Parameters Obtained by the Regression of Flow Curves to Describe the GMD at 600 °C

Mean GS	State Variable	34 Pct β	48 Pct β	64 Pct β
~3 μm	log σ^*	3.11	3.12	3.13
	log $\dot{\alpha}^*$	−3.174	−3.052	−2.748
~11 μm	log σ^*	3.05	3.02	2.96
	log $\dot{\alpha}^*$	−4.608	−4.646	−4.753
		p = **0.15**		

B. *Flow Behavior at 800 °C with the Variation of α/β Phase Ratio and Grain Size*

Figure 4(a) shows the results of the load relaxation test conducted at 800 °C for the fine-grain-size microstructure (3 μm). As compared with the curves in Figure 3, the change of curvature is noted in the strain-rate range of 10^{-5} to 10^{-3} s^{-1}, which is believed to be associated with the occurrence of the P/GBS. In this range, flow stress minima[13] are seen at the 48-pct β microstructure with a 3-μm grain size. However, in the case of the coarse-grained material (11 μm), the effect of β volume fraction on the flow stress is less effective, and no stress minima are observed in Figure 4(b). This is, presumably, due to the decrease of boundary sliding effect in a coarse-grained material in the entire strain-rate region. Here, the different tendencies of flow stress variation with the β volume fraction, *e.g.*, converging at a high-strain-rate region in 3-μm specimens and *vice versa* in 11-μm specimens, is also observed in the curves of 800 °C.

In order to verify whether the theory of inelastic deformation can reasonably explain the deformation behavior of 3-μm-grain materials at 800 °C, the experimental data in Figure 4(a) have been attempted to fit with the calculated curves. Since it is thought that the deformation at 800 °C includes both GMD and P/GBS, the contribution of each deformation mode has been distinguished in the analysis. After the regression of flow curves for fine-grained materials (Figure 4(a)), the GMD and P/GBS curves for the specimens having different α/β phase ratios have been determined, as shown in Figure 5, the corresponding constitutive parameters are obtained from Eqs. [3] and [5], respectively (Table IV). In Figure 5, the narrow solid line represents the portion of GMD and the dashed line denotes that of the P/GBS. The composite curve of the GMD and P/GBS is the thick solid line, which shows good agreement with the experimental values for all microstructures. It is interesting to note that the amounts of overlap between the GMD and P/GBS curves vary with the variation of α/β volume fraction. In the 48-pct β microstructures containing the greatest amount of α/β boundary, the contribution of the P/GBS curve in the whole flow curve is the largest, resulting in the lowest friction stress (Σ_g) in Table IV.

It is also noted in Table IV that the boundary sliding is characterized by a viscous flow process with a power-index

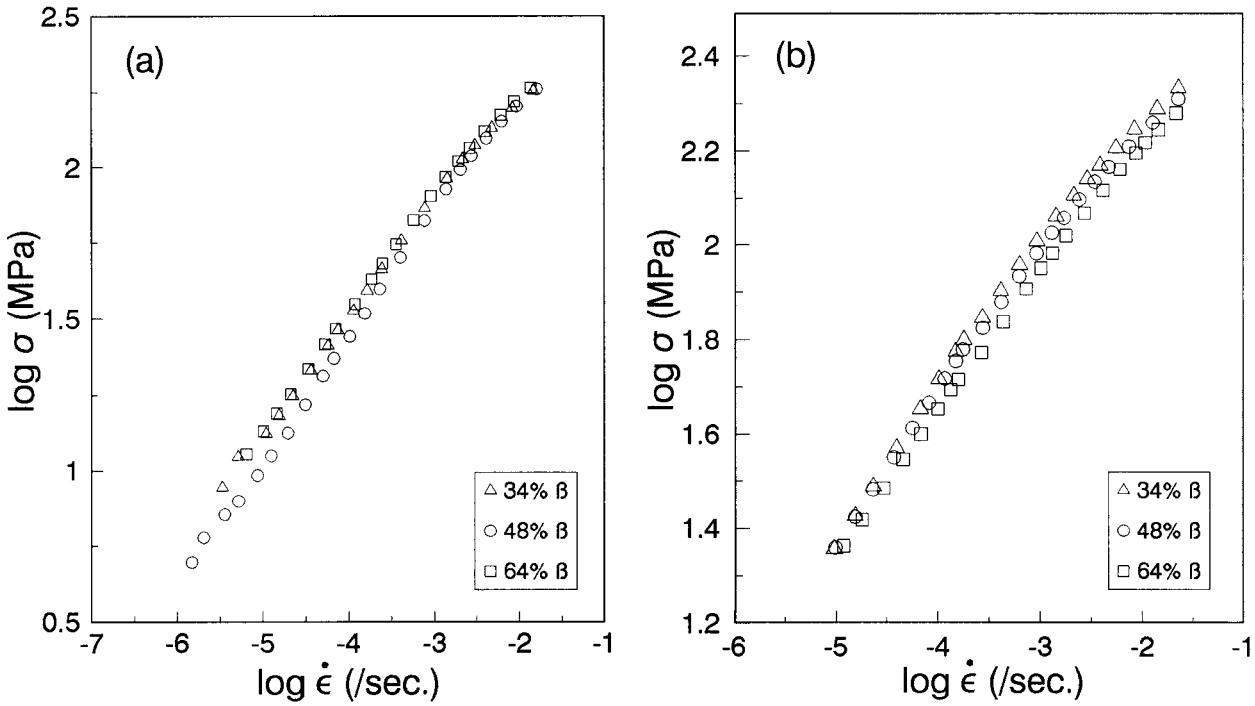

Fig. 4—Effects of β volume fraction on the flow stress curves including GMD and P/GBS for 3-μm and 11-μm-grained microstructures at 800 °C: (*a*) 3-μm microstructure and (*b*) 11-μm microstructure.

value (M_g) of 0.5. This M_g value of 0.5 is lower than the previously reported one ($M_g = 1.0$) for various single-phase Al alloys.[24] However, the value of 0.5 is also observed in other two-phase Pb-Sn[25] and Ti3Al-*x*Nb[26] alloys. Considering $1/M_g$ as a stress exponent, this result also coincides with the Hashimoto's PBS equation $v = \tau^2$ (where v is the PBS velocity and τ is the applied stress), obtained from the bicrystal shear tests.[16] It appears that PBS is responsible for the superplastic deformation of two-phase alloys, resulting in the difference in the M_g values between the single-phase Al alloys and the two-phase Ti alloys.

C. *Measurement of Boundary Sliding Displacements*

For the estimation of the surface displacement at each type of boundary, the scratched specimen was elongated 3 pct (Figure 6(a)) and 30 pct (Figure 6(b)) at 800 °C, respectively, with a strain rate of 10^{-3} s^{-1}, and then quenched by water. Typical surface features of the specimen containing a 34 pct β volume fraction are shown in Figure 6. The slightly lighter region in these micrographs is found to be the β phase, and the tensile axis (T) is parallel to the scratch direction. In Figure 6(a) and (b), as mentioned in Section III, the change of volume ratio (34 pct β) is not observed due to the short period (2 to 8 minutes, respectively) of exposure at a high temperature (800 °C). However, it is seen in Figure 6(b) that a dynamic grain growth has slightly occurred due to the relatively large strain ($\varepsilon = 0.3$) imposed on the specimen.

It is noted in Figure 6(a) that the unique sliding boundary, labeled C, is the α/β phase boundary, and the angle between the sliding direction and the tensile axis is about 45 °. More clear evidence for PBS, labeled C, is shown in Figure 6(b) by the shifts in the longitudinal marker lines. However, unlike the previous prediction by Partridge *et al.*,[5] α/α boundary slidings (point A) are frequently seen, while the β/β boundary slidings (point B) are not easily observed. It is also noted that the scratched lines in the interior of the β phase are more deflected than those in α phase, presumably due to heavy deformation of the β grains (point D), and that a new grain has emerged from the interior of the specimen (point E) due to the increase of surface area.[14]

V. DISCUSSION

A. *Matrix Deformation Mode in the Two-Phase ($\alpha + \beta$) Ti-6Al-4V Alloy*

It is worthwhile to discuss here how the deformation behavior in the two-phase ($\alpha + \beta$) Ti-6Al-4V alloy is related to the deformation behavior of each constituent phase, *e.g.*, α or β phase at high temperature, since it can provide an insight into the accommodation mechanism as well as the matrix deformation mechanism. In general, there are two limiting modes for describing the deformation of two-phase alloys, each described by a rule-of-mixture relationship. One is an isostrain-rate mode, where there is a stress distribution between the α and β phases such that the resultant matrix deformation rates or the accommodation rates in the two phases are equal. The other is an isostress mode, where the stresses in the α and β phases are assumed to be equal, resulting in a strain-rate distribution between the two phases. Since the β phase in the $\alpha + \beta$ titanium alloys represents considerably lower flow stress than the α phase, the deformation of the β phase is constrained by the α phase in the isostrain-rate mode, and consequently, the overall matrix deformation characteristics are mainly controlled by the α phase. However, in the isostress mode, the

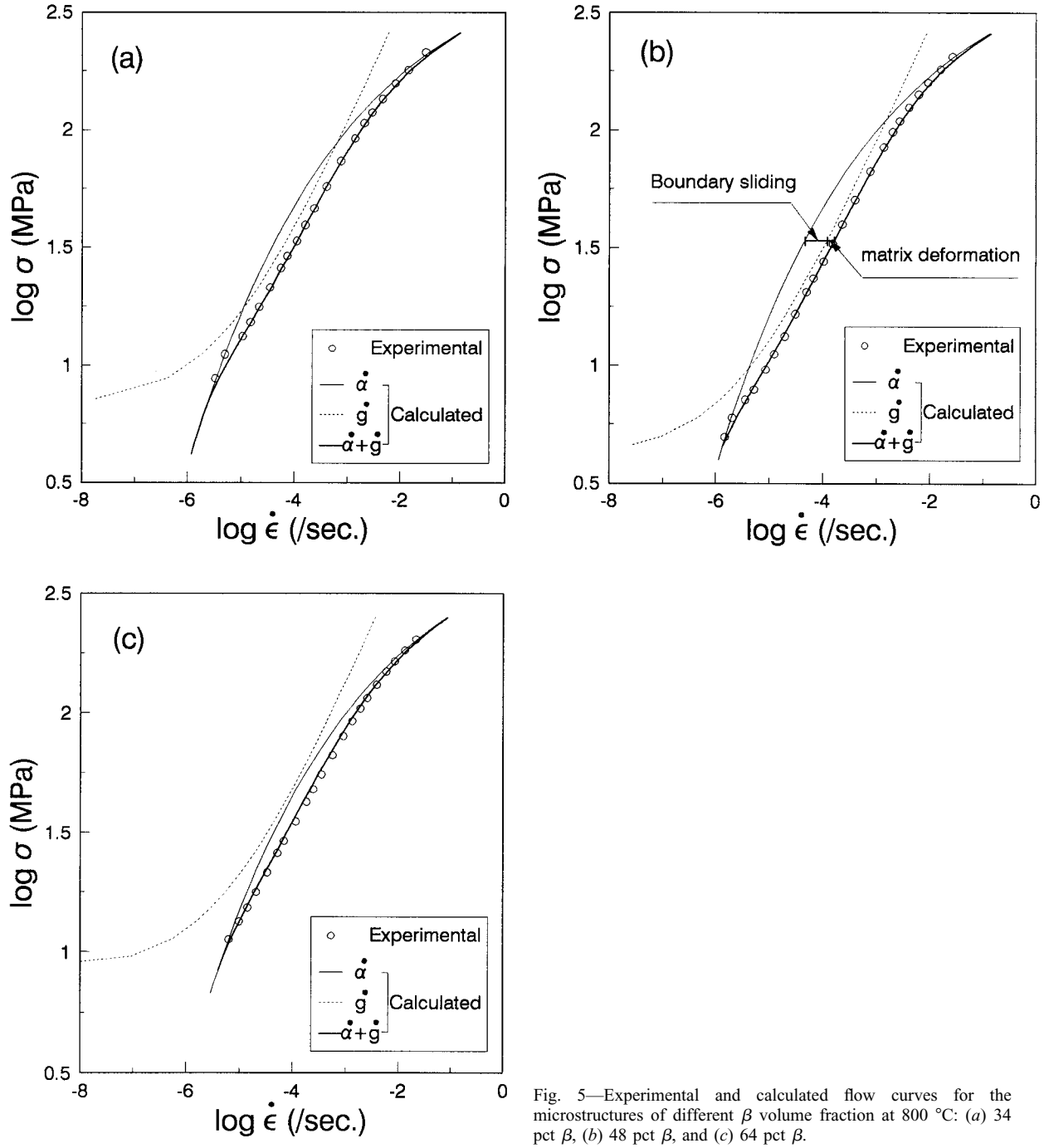

Fig. 5—Experimental and calculated flow curves for the microstructures of different β volume fraction at 800 °C: (*a*) 34 pct β, (*b*) 48 pct β, and (*c*) 64 pct β.

overall matrix deformation is, rather, controlled by the deformation of the β phase.

In describing the superplastic deformation behavior of the Ti-6Al-4V alloy, there has been an argument over the corresponding deformation mode. The only experimental work directed at that matter has been carried out by Hamilton *et al.*,[7] and the data fit well with the isostrain-rate mode, implying that the overall matrix deformation is controlled by the α phase. However, Leader *et al.*[8] have shown that the isostress mode is more appropriate and predicts better the effect of the addition of β-stabilizing elements in the Ti-6Al-4V alloy. Recently, Meier *et al.*[9] suggested that actual behavior may follow the composite mode of these two modes. It is thought that these controversies arise mainly due to the combined phenomenon of the GBS or phase boundary sliding (PBS) and the accommodation process occurring concurrently during superplastic deformation.

In this work, in order to investigate solely the matrix deformation mode and/or accommodation mode, the internal strength (σ^*) and its conjugate reference strain rate ($\dot{\alpha}^*$) of GMD for coarse- and fine-grained materials are normalized, and presented in Figure 7. The isostress and isostrain-rate modes constitute the upper and lower bounds of the deformation, and consequently, all the deformation modes are in the range of these two modes.[9] It is interesting to note that the deformation mode of fine-grained material (3 μm) is different from that of coarse-grained

Table IV. Constitutive Parameters Obtained by the Regression of Flow Curves for 3-μm Grained Materials to Describe the GMD and P/GBS Occurring at 800 °C

State	34 Pct	48 Pct	64 Pct
Variable	β	β	β
Log σ^*	2.79	2.79	2.83
Log $\dot{\alpha}^*$	−1.272	−1.265	−1.125
	p = **0.15**		
Log $\dot{g}_0$	−5.36	−5.65	−5.36
Σ_g	0.826	0.615	0.923
	M_g = **0.5**		

material (11 μm). In the case of the 3-μm size, the deformation behavior is close to the isostress mode, implying that the GMD is primarily governed by the β phase (at 600 °C) and that the boundary sliding is mostly accommodated by the β phase (at 800 °C). It also coincides with the fact that the scratched lines in the interior of the β phase are more deflected than those of the α phase, due to the heavy deformation of β grains (point D), as shown in Figure 6. However, the deformation of the 11-μm-grain microstructure at 600 °C represents the mixed type between isostress and isostrain-rate modes, which agrees well with the work of Meier *et al.*[9] It implies that the deformation of α phase increases with the increase of grain size. This is interpreted in association with the different stress concentrations in small- and large-grained materials; as such, the increase of β grain size results in a larger slip distance and a heavy stress concentration at the grain boundary, which makes it easy to deform the adjacent α grains.

B. *Relative Resistance between GBS and PBS*

Since the two-phase alloys contain both the grain boundary and the phase boundary in the microstructure, PBS can also occur along with GBS during superplastic deformation. As to the relative ease of each boundary sliding, not much information is available in the literature. Considering that the superplastic deformation behavior of two-phase Ti-6Al-4V alloys is largely affected by the α/β phase ratio, it is apparent that the relative sliding resistances of α/α, α/β, and β/β boundaries are different from each other. In the present study, the values of static friction stress (Σ_g), an indication of sliding resistance, of all the boundaries are measured and represented in Table IV. It is important to note in Table IV that the static friction stress is the lowest in the 48-pct β microstructure which contains the maximum α/β boundaries, and increases, in order, with the 34 pct β (having more α/α boundaries) and the 64 pct β (having more β/β boundaries) microstructures. This indicates that the critical stress for boundary sliding is the lowest in the α/β boundary and, subsequently, that the α/β PBS governs the overall deformation, resulting in the maximum elongation in the 48-pct β microstructure.

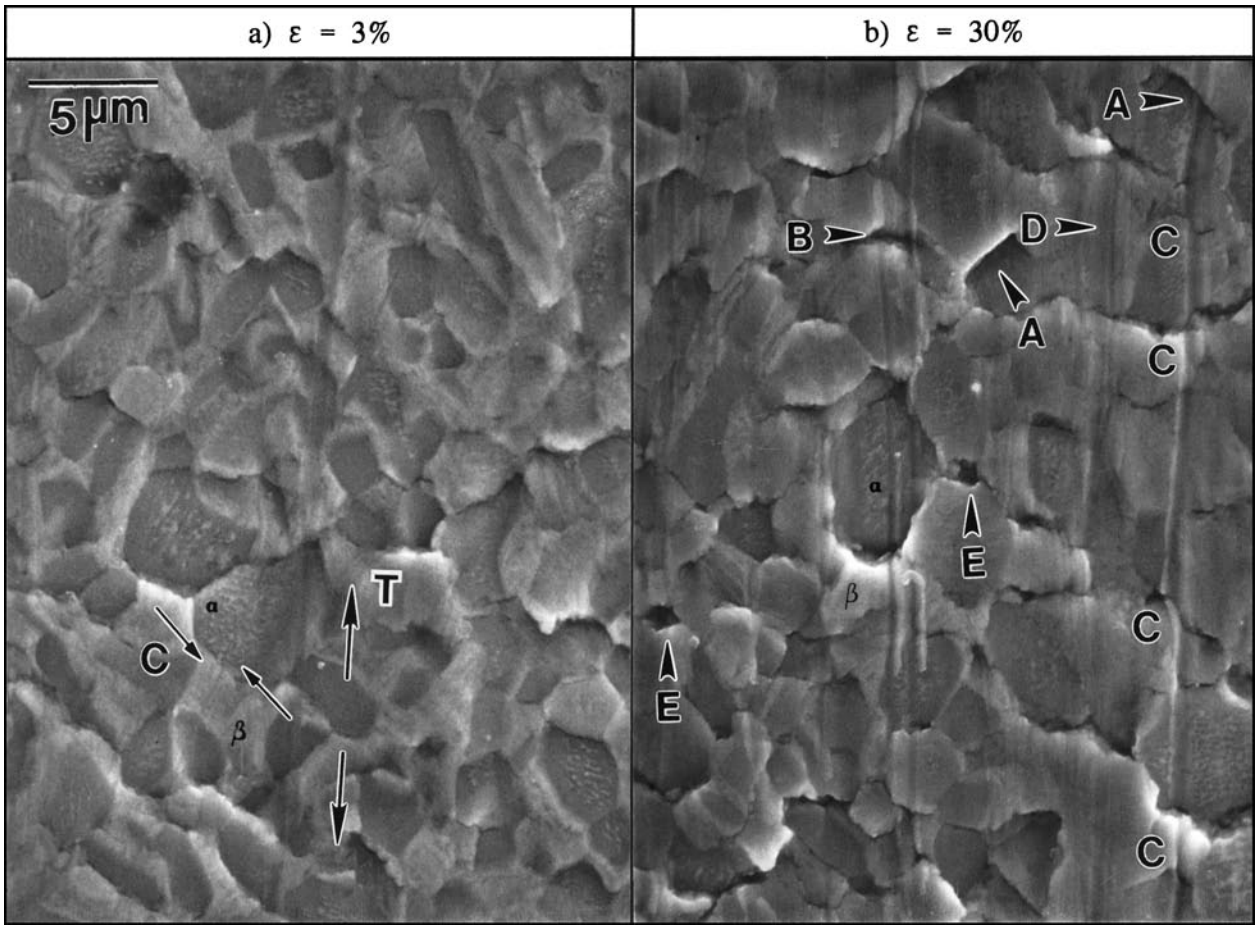

Fig. 6—The gage surface of the specimen elongated to (*a*) 3 pct and (*b*) 30 pct with an initial strain rate of 10^{-3} s^{-1} for the microstructure of 34 pct β volume fraction.

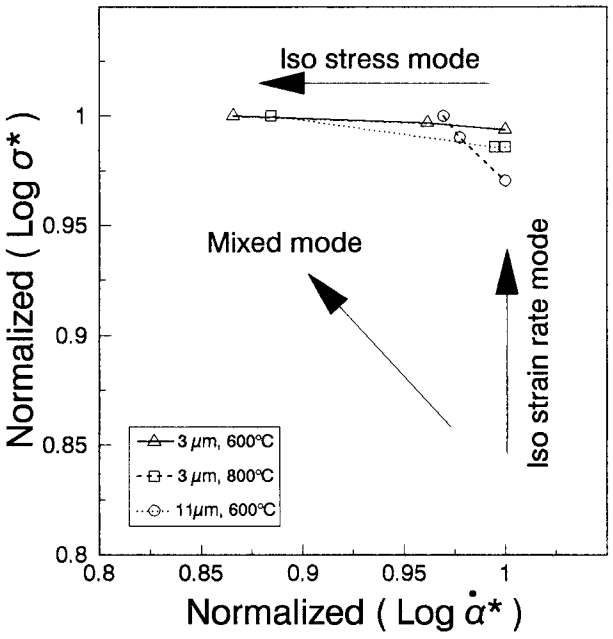

Fig. 7—Determination of deformation mode occurring at 600 °C and 800 °C.

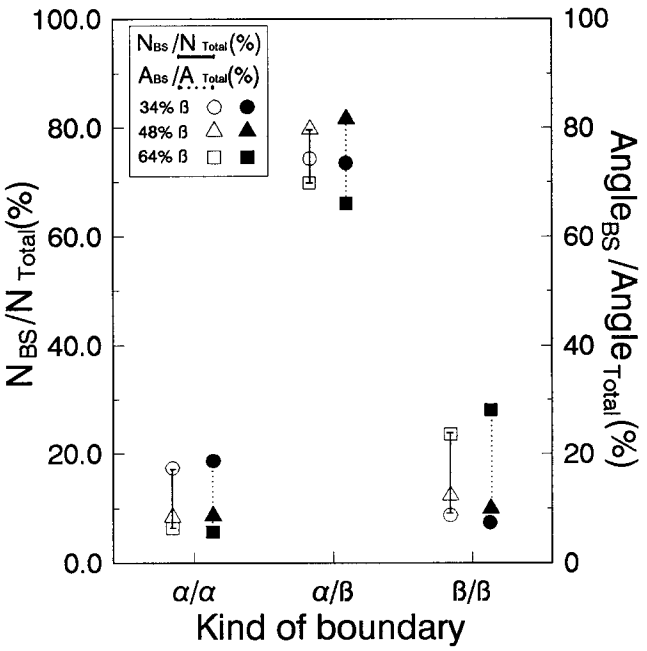

Fig. 8—The amounts of boundary slidings measured in the specimens elongated up to 30 pct.

Our results, however, differ from those obtained by others,[5,27] where the sliding resistance is predicted to increase on the order of $\alpha/\beta \leq \beta/\beta << \alpha/\alpha$ or $\beta/\beta \leq \alpha/\beta << \alpha/\alpha$. The discrepancy is thought to result from the following two reasons. First, they have assumed that the sliding rate is proportional to the grain boundary diffusion coefficient (D_{gb}), which is subsequently proportional to the bulk diffusion coefficient. Therefore, their analysis is mainly based upon the diffusion-based mechanism and uses the flow stress data obtained from several Ti alloys. Second, they have used a contiguous α-phase microstructure consisting of low-angle boundaries, where the α/α boundary sliding rate is expected to be lower as compared with that of high-angle boundaries.[11] Since our study has been carried out using equiaxed microstructures, the α/α boundary sliding is more easily seen to operate in the microstructure, as shown in Figure 6.

To confirm the previous analysis on the relative sliding resistance of boundaries, the amounts of each boundary sliding are measured from the surface photomicrographs and are presented in Figure 8. It is clear that the PBS is predominant in all three microstructures, with different β volume fractions ranging from 65 to 83 pct of the overall deformation. It is also seen that the 34 pct β and 64 pct β microstructures, in which the boundaries of α/α and β/β are increased, represent increased portions of α/α and β/β boundary sliding, respectively, to maintain the continuity and compatibility between the grains. It appears that the enhancement of GBS is more effective in the β/β boundaries than the α/α boundaries, due to the high wettability of the β phase.[5] From the previous analysis and observation, it is concluded that the sliding resistance for the different types of boundaries is ranked as $\alpha/\beta << \text{M}\ \alpha/\alpha \approx \beta/\beta$.

C. *Effects of β Volume Fraction on GMD and P/GBS*

Since the inelastic deformation theory includes both GMD and P/GBS, the effects of the α/β phase ratio on each mode can be separately considered in this section Figure 9(a) represents the effect of an increasing β volume fraction on the flow curves of the P/GBS mode for 3-μm microstructures at 800 °C. It is noticed that the shift of the curves with the variation of β volume fraction is significant in the whole strain-rate region and shows the largest discrepancy at the lower-strain-rate region. Also, the flow stress curve of P/GBS is at a minimum in the 48-pct β microstructure, which contains mainly the α/β phase boundaries representing the lowest sliding resistance. The stress minima[13] generally observed in the dual-phase titanium alloy are mainly attributed to the different flow stresses for PBS and GBS.

On the other hand, the effect of the β volume fraction on the flow curves of the GMD mode is not noteworthy, although a slight variation in the flow curves occurs with an increase in the β volume fraction, as shown in Figure 9(b). It is interesting to note that the decreasing order of flow stress for GMD is different from that of P/GBS, such that the flow stress for GMD decreases with an increase in the β volume fraction. This indicates that the increase of β volume fraction contributes to lowering the flow stress for GMD as well as the accommodation of P/GBS at 800 °C. However, the effects are insignificant. It is, therefore, considered that the major effect of varying the β volume fraction is to change the flow stress of P/GBS, mainly due to the variations in the number of α/α, α/β, and β/β boundaries, which possess different levels of sliding resistance. The fact that in a coarse-grained (11 μm) microstructure, where the P/GBS is less predominant (Figure 4(b)) than the fine-grained (3 μm) microstructure (Figure 4(a)), the variation of flow stress with the β volume fraction is insignificant, especially in the strain-rate region of 10^{-5} to 10^{-3} s^{-1}, supports the previous interpretation.

From the previous results, the optimum α/β ratio to obtain the best superplasticity in a Ti-6Al-4V alloy is consid-

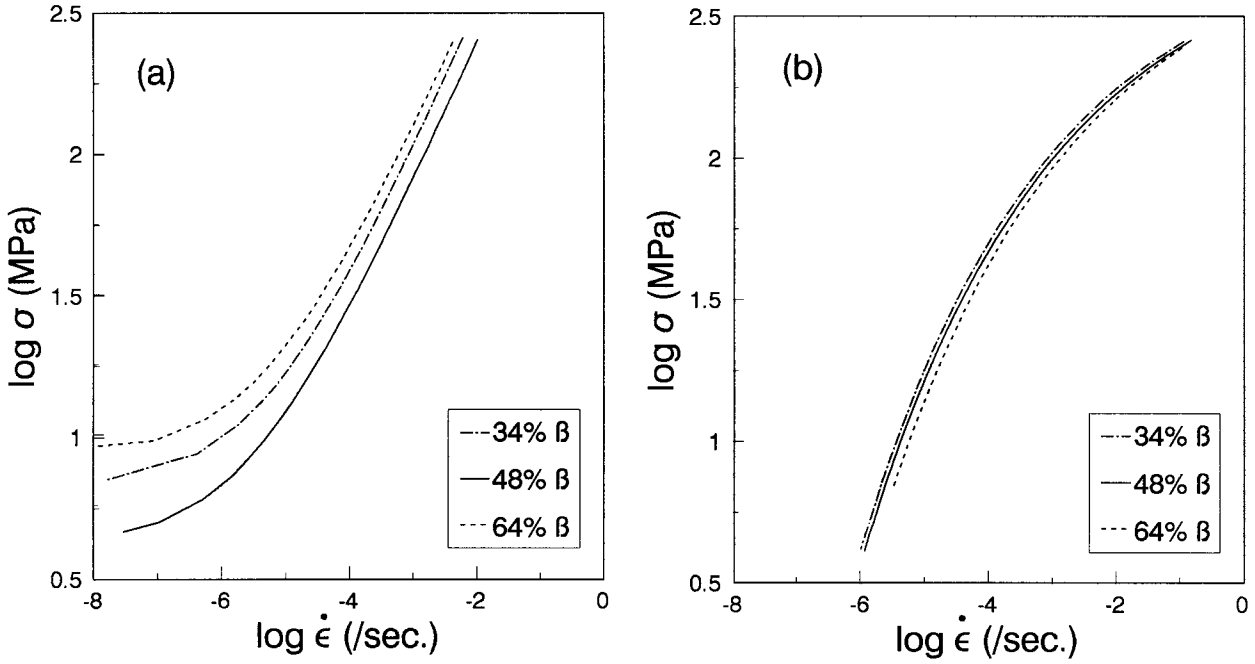

Fig. 9—The variation of GMD and P/GBS curves with the β volume fraction at 800 °C: (*a*) P/GBS curves and (*b*) GMD curves.

ered to be about 50 · 50; similar portions (40 to 50 pctβ) are also suggested by the earlier work.[28] However, this optimum volume ratio is found to vary in other two-phase titanium alloys: 60 to 70 pct β in several near-β titanium alloys,[29,30] approximately 25 pct β in Ti_3Al-Nb alloys[31] and 50 pctβ in TiAl alloys,[32] which is presumably to be associated with the grain growth behavior of each alloy system. Therefore, in order to predict the optimum volume ratio in dual-phase alloys, it is suggested that the grain growth behavior of the alloy should also be considered along with the details of the boundary sliding characteristics and the matrix deformation behavior.

VI. CONCLUSIONS

1. The overall deformation characteristics of the Ti-6Al-4V alloy with the variation of α/β volume fraction (34, 48, and 64 pctβ) and grain size (3 and 11 μm) at 600 °C and 800 °C are well described by the inelastic deformation theory.
2. The GMD mode is found to be dominant at 600 °C and its flow curves are fitted well with the plastic-state equation when a permeability parameter (p) is 0.15. The PBS mode becomes dominant at 800 °C and its flow curves are consistent with the viscous flow equation, with $M_g = 0.5$.
3. The mode of GMD for the fine-grained structures (3 μm) well agrees with the isostress model, while that for the coarse-grained materials (11 μm) is found to be a mixed type of both isostress and isostrain-rate modes.
4. The sliding resistance of different boundaries is increased on the order of $\alpha/\beta << \alpha/\alpha \approx \beta/\beta$. The largest elongation, observed in the 48 pct β structure, is primarily attributed to the maximum number of α/β phase boundaries, which possess the lowest sliding resistance.
5. With the variation of the α/β phase ratio, the flow stress curves for P/GBS are significantly shifted as compared to those for GMD, which influences greatly the overall superplastic deformation.

ACKNOWLEDGMENTS

The authors are grateful to the Korean Ministry of Education for their financial support through a research project for Advanced Materials in 1995.

REFERENCES

1. E.D. Weisert and G.W. Stacher: in *Superplastic Forming of Structural Alloys*, N.E. Paton and C.H. Hamilton, eds., TMS-AIME, Warrendale, PA, 1982.
2. S.B. Lee, JS Kim, W.Y. Chang, and C.S. Lee: *Proc. 3rd Japan Int. SAMPE Symp.*, TMS, Warrendale, PA, 1993, pp. 1946-53.
3. A.K. Ghosh and R. Raj: *Acta Metall.*, 1981, vol. 29, pp. 607-16.
4. A.K. Ghosh and C.H. Hamilton: *Metall. Trans. A*, 1979, vol. 10, pp. 699-706.
5. P.G. Partridge, D.S. Mcdarmaid, and A.W. Bowen: *Acta Metall.*, 1985, vol. 33, pp. 571-77.
6. J.A. Wert and N.E. Paton: *Metall. Trans. A*, 1983, vol. 14A, pp. 2535-44.
7. C.H. Hamilton, A.K. Ghosh, and M.M. Mahoney: in *Advanced Processing Methods for Titanium*, C.H. Hamilton and D.F. Hasson, eds., TMS-AIME, Warrendale, PA, 1982, pp. 129-44.
8. J.R. Leader, D.F. Neal, and C. Hammond: *Metall. Trans. A*, 1986, vol. 17A, pp. 93-106.
9. M.L. Meier, D.R. Lesuer, and A.K. Mukherjee: *Mater. Sci. Eng.*, 1991, vol. A136, pp. 71-78.
10. B. Baudelet: *Mater. Sci. Eng.*, 1991, vol. A137, pp. 41-55.
11. J.W. Edington, K.N. Melton, and C.P. Cutler: *Prog. Mater. Sci.*, 1976, vol. 21, pp. 61-158.
12. M.L. Meier, D.R. Lesuer, and A.K. Mukherjee: *Mater. Sci. Eng.*, 1992, vol. A154, pp. 165-73.
13. A. Dutta and D.S. Kumar: *Mater. Sci. Eng.*, 1995, vol. A194, pp. L1-L4.
14. T.G. Langdon: *Mater. Sci. Eng.*, 1994, vol. A174, pp. 225-30.
15. Z.R. Lin, A.H. Chokshi, and T.G. Langdon: *J. Mater. Sci.*, 1988, vol. 23, pp. 2712-22.
16. S. Hashimoto, F. Moriwaki, T. Mimaki, and S. Miura: in

Superplasticity in Advanced Materials, S. Hori, ed., ICSAM, Osaka, Japan, 1991, pp. 23-32.
17. A. Eberhardt and B. Baudelet: *Phil. Mag.*, 1980, vol. A41, pp. 843-69.
18. Y.W. Chang and E.C. Aifantis: in *Constitutive Laws for Engineering Materials: Theory and Application*, C.S. Desai, ed., Elsevier, Tucson, AZ, 1987, pp. 293-300.
19. L.E. Malvern: *Introduction Mechanics of a Continuous Media*, Prentice-Hall, Englewood Cliffs, NJ, 1969, pp. 401-02.
20. E.W. Hart: *Trans. ASME*, 1984, vol. 106, pp. 322-25.
21. M. Peters: *Z. Metallk.*, 1983, vol. 74, pp. 274-82.
22. E.W. Hart: *J. Eng. Mater Technol.*, 1976, pp. 193-202.
23. T.K. Ha, C.S. Lee, and Y.W. Chang: *Scripta Mater.*, 1996, vol. 35, pp. 635-40.
24. T.K. Ha and Y.W. Chang: *Scripta Mater.*, 1995, vol. 32, pp. 809-14.
25. T.K. Ha and Y.W. Chang: *Scripta Mater.*, 1996, vol. 35, pp. 1317-23.
26. J.S. Kim and C.S. Lee: in *Titanium 95*, P.A. Blenkinsop, ed., The Institute of Materials, Birmingham, U.K., 1995, vol. 1, pp. 356-63.
27. S.M.L. Sastry, P.S. Pao, and K.K. Sankaran: *Titanium 80, Science and Technology*, H. Kimura and O. Izumi, eds., AIME, New York, NY, 1980, vol. 2, pp. 873-86.
28. M.T. Cope, D.R. Evetts, and N. Ridley: *J. Mater. Sci.*, 1986, vol. 21, pp. 4003-08.
29. Pan Ya Qin, Liu Weimin, and Song Zuozhou: in *Superplasticity and Superplastic Forming*, C.H. Hamilton and N.E. Paton, eds., TMS, Warrendale, PA, 1988, pp. 263-67.
30. E. Girault, J.J. Blandin, A. Varloteaux, M. Suery, and Y. Combres: *Scripta Mater.*, 1993, vol. 29, pp. 503-06.
31. A. Dutta and D. Banerjee: *Scripta Mater.*, 1990, vol. 24, pp. 1319-22.
32. W.B. Lee, H.S. Yang, Y.W. Kim, and A.K. Mukherjee: *Scripta Mater.*, 1993, vol. 29, pp. 1403-08.